

Site-specific tagging proteins with a rigid, small and stable transition metal chelator, 8-hydroxyquinoline, for paramagnetic NMR analysis

Yin Yang¹ · Feng Huang¹ · Thomas Huber² · Xun-Cheng Su¹

Received: 18 November 2015 / Accepted: 1 January 2016 / Published online: 6 January 2016
© Springer Science+Business Media Dordrecht 2016

Abstract Design of a paramagnetic metal binding motif in a protein is a valuable way for understanding the function, dynamics and interactions of a protein by paramagnetic NMR spectroscopy. Several strategies have been proposed to site-specifically tag proteins with paramagnetic lanthanide ions. Here we report a simple approach of engineering a transition metal binding motif via site-specific labelling of a protein with 2-vinyl-8-hydroxyquinoline (2V-8HQ). The protein-2V-8HQ adduct forms a stable complex with transition metal ions, Mn(II), Co(II), Ni(II), Cu(II) and Zn(II). The paramagnetic effects generated by these transition metal ions were evaluated by NMR spectroscopy. We show that 2V-8HQ is a rigid and stable transition metal binding tag. The coordination of the metal ion can be assisted by protein sidechains. More importantly, tunable paramagnetic tensors are simply obtained in an α -helix that possesses solvent exposed residues in positions i and $i + 3$, where i is the residue to be mutated to cysteine, $i + 3$ is Gln or Glu or $i - 4$ is His. The coordination of a sidechain carboxylate/amide or imidazole to cobalt(II) results in different structural geometries, leading to different paramagnetic tensors as shown by experimental data.

Keywords Protein labeling · 8-Hydroxyquinoline · Paramagnetic NMR spectroscopy · Pseudocontact shift · Paramagnetic relaxation enhancement

Introduction

One of the mainstream uses of transition metals in structural biology is exploiting the diverse paramagnetic properties of these ions (Bertini and Luchinat 1996, 1999; Clore and Iwahara 2009) by high resolution NMR spectroscopy. The intrinsic paramagnetic properties of transition metal ions provide valuable structural restraints in biomolecules, which are governed by the well-established theory (Abragam and Bleaney 1970; La Mar et al. 1973; Bertini and Luchinat 1996). These paramagnetic effects, including paramagnetic relaxation enhancement (PRE), pseudocontact shift (PCS) and residual dipolar coupling (RDC), are experimentally observable by NMR spectroscopy. In particular, PCSs as the chemical shift differences between the paramagnetic and diamagnetic species can be measured with high accuracy. While PREs only depend on the distance between the paramagnetic center and the observed nuclear spins, PCSs contain both distance and direction information of the nuclear spins with respect to the paramagnetic center (Bertini et al. 2002; Clore and Iwahara 2009; Otting 2010). Because of their high chemical similarity and large variations in the paramagnetic anisotropy, lanthanide ions have received increasing interests in structural biology by means of high resolution NMR spectroscopy (Geraldes 1993; Bertini et al. 2002; Geraldes and Luchinat 2003; Pintacuda et al. 2007; Otting 2008; Bertini et al. 2008; Otting 2010; Liu et al. 2014). As many proteins do not contain a paramagnetic center, strategies for site-specific labeling of proteins with paramagnetic species

Electronic supplementary material The online version of this article (doi:10.1007/s10858-016-0011-7) contains supplementary material, which is available to authorized users.

✉ Xun-Cheng Su
xunchengsu@nankai.edu.cn

¹ State Key Laboratory of Elemento-Organic Chemistry, Collaborative Innovation Center of Chemical Science and Engineering (Tianjin), Nankai University, Tianjin 300071, China

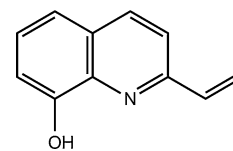
² Research School of Chemistry, Australian National University, Canberra, ACT 0200, Australia

have been developed (Rodríguez-Castañeda et al. 2006; Su and Otting 2010; Koehler and Meiler 2011; Liu et al. 2014). Paramagnetic transition metal ions have an even longer history in paramagnetic protein NMR spectroscopy (La Mar et al. 1973; Bertini and Luchinat 1984; Bertini et al. 1993; Bertini and Luchinat 1996; Donaire et al. 1998; Ubbink et al. 1998; Bertini et al. 2005; Jensen et al. 2004; Arnesano et al. 2005), however, site-specific labeling of biomolecules with a rigid transition metal ion is less studied (Gochin 1998; Man et al. 2010; Nguyen et al. 2011). Complexes of high-spin Co(II) produce the largest paramagnetic anisotropy and Mn(II) complexes exert strong PRE effects on nuclear spins because Mn(II) has five unpaired electrons and usually a long electronic relaxation time (Bertini and Luchinat 1996). Cu(II) forms more stable complexes but generally generates weaker PREs than Mn(II). In the case of Ni(II), its paramagnetic effects are largely determined by its coordination with the chelating ligand. In comparison with lanthanide ions, transition metal ions have fewer coordination sites (generally up to six) and prefer to coordinate with histidine sidechains. This offers additional advantages in the design of smaller and more rigid paramagnetic tags, as the stability and rigidity of the tag strongly influences the interpretation of paramagnetic restraints from NMR spectroscopy.

8-Hydroxyquinoline (8HQ), a frequently used organic chelator for metal ions, forms stable complexes with transition metal ions in varying molar ratio (Johnston and Freiser 1952). Incorporation of 8HQ into a protein via bioorthogonal protein synthesis has recently been reported (Lee et al. 2009; Liu et al. 2013; Park et al. 2015). However, 8HQ is a bidentate ligand, i.e. it has only two coordinating atoms. Therefore, one 8HQ moiety alone is not able to immobilize the metal ion without additional coordination by the protein, and aggregation due to the unsaturated coordination sites of the metal ion should be prevented in the design of paramagnetic tags for NMR or other spectroscopic analysis in structural biology. Several examples have shown that simultaneous coordination by a protein sidechain and a small functional tag can avert the tag-induced protein aggregation and significantly restrain the metal ion, thus suppressing the positional fluctuations of the paramagnetic center (Su et al. 2008; Swarbrick et al. 2011; Yagi et al. 2013; Huang et al. 2013).

The high reactivity and chemoselectivity of a 4-vinyl pyridine moiety to thiol groups of proteins has been demonstrated in protein modifications for paramagnetic NMR and EPR analysis (Li et al. 2012; Yang et al. 2013; Qi et al. 2014; Martorana et al. 2015). We herein report an 8HQ derivative, 2-vinyl-8-hydroxyquinoline (2V-8HQ), which can be site-specifically attached to a protein via a Michael addition-like thiol-ene reaction (Fig. 1 and Scheme 1). To test the reactivity of 2V-8HQ to protein thiols, we made two single-point cysteine mutants of human ubiquitin, T22C and

Fig. 1 Molecular structure of 2V-8HQ



A28C, respectively. The combination of a small functional tag and protein sidechain in immobilizing the transition metal ions was analyzed. The rigidity of the transition metal ion with respect to the protein and the affinity of sidechains of glutamate, glutamine and histidine for the metal ion were evaluated by high resolution NMR spectroscopy and isothermal titration calorimetry (ITC). In the structure of ubiquitin, the solvent exposed sidechains of residues Glu24, Gln31 and Asp32 are close to Thr22 and Ala28, respectively, and can assist in binding a metal ion in addition to 8HQ. As imidazole is a preferred ligand for transition metal ions, the double-point mutant E24H/A28C was constructed. The PCSs of A28C-2V-8HQ and E24H/A28C-2V-8HQ complexed with Co(II) differed significantly, suggesting different paramagnetic tensors. Tunable paramagnetic anisotropy is highly valuable in structural biology, and we show that different sets of paramagnetic susceptibility tensors can simply be obtained by changing the metal ion coordination by straight-forward protein sidechain mutagenesis.

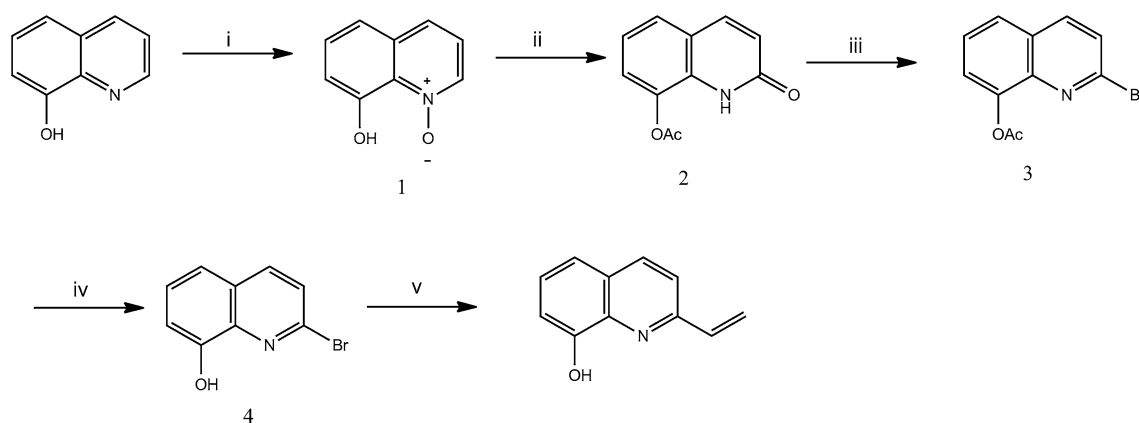
Materials and methods

Protein expression and purification

The target proteins were expressed using an optimized high-density method (Cao et al. 2014) according to the previously reported protocol (Marley et al. 2001) and typically 20 mg ^{15}N -protein was obtained from 250 mL M9 media.

Synthesis of 2V-8HQ

N-oxide-8-hydroxyquinoline (1): 0.5 g 8-hydroxyquinoline was dissolved in 4 mL dichloromethane and 0.69 g *meta*-chloroperbenzoic acid (*m*-CPBA) was added stepwise in an ice-cooled water bath. The resulting mixture was stirred at room temperature overnight. 7.14 mL 2 M NaOH was added slowly to the above solution. The organic layer was separated and the water phase was washed with dichloromethane. The organic fractions were combined and washed with brine, dried with sodium sulfate, and then filtered. The organic solvent was removed under reduced pressure, resulting in 0.39 g title compound as yellow solid (yield, 70.3 %) ^1H NMR (300 MHz, CDCl_3) δ 8.25 (dd, $J = 6.0, 0.8$ Hz, 1H), 7.80 (d, $J = 8.1$ Hz, 1H), 7.50 (t, $J = 8.0$ Hz, 1H), 7.25–7.21 (m, 2H), 7.08 (dd, 1H).



Scheme 1 Reagents and conditions: *i* *m*-CPBA/DCM, *ii* Ac₂O/Ar/100 °C, *iii* POBr₃/Ar/CHCl₃, *iv* hydrolysis, *v* triethoxyvinylsilane/Pd(OAc)₂/TBAF/PPh₃/DMF

Compounds 2, 3 and 4 were synthesized according to the published methods with minor modifications (Petitjean et al. 2005).

2-Vinyl-8-hydroxyquinoline (2V-8HQ): similar to the previously reported coupling reaction (Alacid and Najera 2008), the mixture of 1.2 g (0.03 mol) NaOH, 20 mg (0.09 mmol) Pd(OAc)₂, 2.28 g (0.01 mol) compound 4, 2.53 mL (0.012 mmol) triethoxyvinylsilane, 30 mL H₂O and 30 g PEG 2000 was stirred at 80–90 °C for 10 h and the resulting mixture was extracted with diethyl ether. The organic phase was combined and washed with brine. The organic solution was dried with sodium sulfate and filtered. The organic solvent was removed under reduced pressure, resulting in 2.0 g title compound as white powder (yield, 88.9 %). ¹H NMR (¹H 400 MHz, CDCl₃) δ 7.95 (d, *J* = 8.6 Hz, 1H), 7.43 (d, *J* = 8.6 Hz, 1H), 7.27 (q, *J* = 8.3 Hz, 1H), 7.15 (d, *J* = 8.2 Hz, 1H), 7.05 (d, *J* = 7.5 Hz, 1H), 6.86 (dd, *J* = 17.7, 10.9 Hz, 1H), 6.18 (d, *J* = 17.7 Hz, 1H), 5.52 (d, *J* = 10.9 Hz, 1H).

NMR experiments

All NMR spectra of protein samples were recorded at 298 K on a Bruker AV600 NMR spectrometer equipped with a QCI-cryoprobe. The protein samples were in 20 mM 2-(*N*-morpholino)ethanesulfonic acid (MES) buffer at pH 6.4 unless indicated otherwise. The recycle delay for PRE measurements was 2 s for both diamagnetic and paramagnetic samples.

Site-specific labeling of ubiquitin mutant with 2V-8HQ

0.5 mM solution of ¹⁵N-labeled protein in 20 mM tris(hydroxymethyl)aminomethane (Tris) pH 7.8 was first mixed with 0.2 mM tris(2-carboxyethyl)phosphine (TCEP), and

then five equivalents of 2V-8HQ (100 mM in ethanol stock solution) were added to the protein solution. It should be noted that excess of TCEP is not desirable as TCEP reacts with vinyl tags. The pH was adjusted to 7.8 using 1.0 M NaOH and the mixture was incubated at room temperature for about 10 h. The ligation product was purified by gel filtration. The overall yield of purified ligation product was approximately 80 %.

Results and discussion

2V-8HQ is a thiol-specific reaction reagent for labeling proteins

The ligation reaction was monitored by recording ¹⁵N-HSQC spectra of the reaction mixture with the ¹⁵N-ubiquitin mutant protein with 2V-8HQ. Quantitative ligation of protein and 2V-8HQ was achieved by incubating the protein with five equivalents of tag at room temperature, pH 7.8 in 20 mM Tris buffer for 10 h. The reaction of 2V-8HQ with the ubiquitin mutants T22C, A28C and E24H/A28C was completed in 10 h at pH 7.8 in 20 mM Tris buffer (monitored by ¹⁵N-HSQC spectra), and the reactivity of 2V-8HQ towards free thiols is significantly higher than the previously reported 4V-PyMTA (Yang et al. 2013) and also 4V-DPA (Li et al. 2012). The tagging reaction rate increases with pH and the ligation can be completed within 5 h at pH 8.5.

Mass analysis by MALDI-TOF mass spectrometry confirmed that proteins were conjugated with only one tag (Fig S2), suggesting no additional groups, including the amino group of the N-terminal methionine and amino groups of lysine sidechains, reacted with 2V-8HQ. This is consistent with NMR chemical shift mapping in ¹⁵N-HSQC spectra using free protein and its 2V-8HQ conjugates (Fig. 2 and

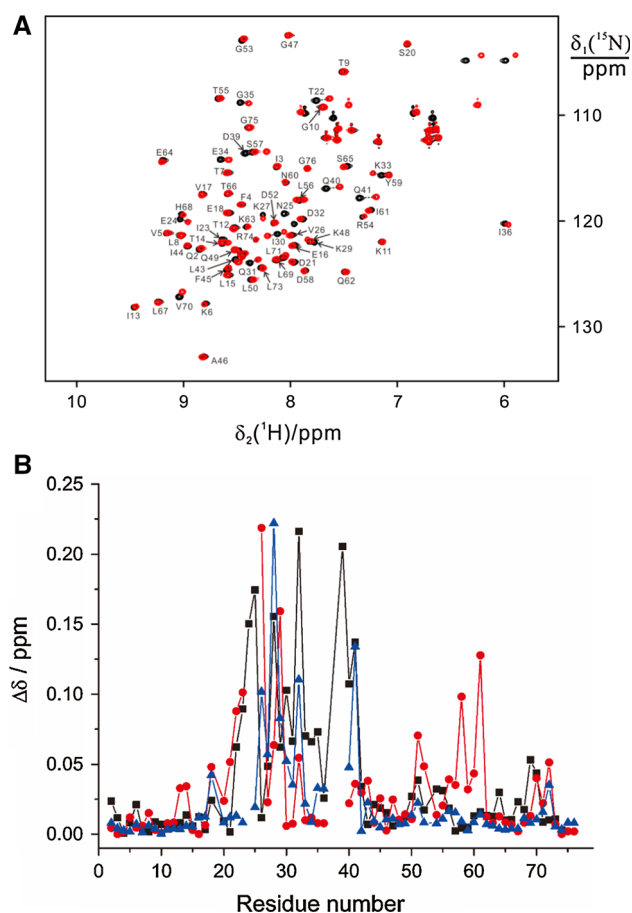


Fig. 2 **a** Superimposition of ¹⁵N-HSQC spectra of 0.1 mM uniformly ¹⁵N-labeled ubiquitin E24H/A28C (black) and E24H/A28C-2V-8HQ conjugate (red). **b** Chemical shift differences $\delta = ((\Delta\delta_{\text{H}})^2 + (\Delta\delta_{\text{N}}/10)^2)^{1/2}$ between free protein and its 2V-8HQ conjugate: T22C (red circles); A28C (blue triangles); E24H/A28C (black squares). Significant chemical shift changes were also observed for residues 50–60 that are close to T22 in the T22C-2V-8HQ adduct

Fig. S1), as the chemical shift perturbations were mainly located around the ligation site of the protein thiol. The high specificity of the reactions of 2V-8HQ with protein thiols suggests that this small tag can be applied to label proteins via the formation of a stable thioether tether.

Interaction of 2V-8HQ protein adducts with transition metal ions

The interactions of transition metal ions with ubiquitin-2V-8HQ adducts were first analyzed by titration of Co(II) into the solution of protein conjugates, because Co(II) has a large magnetic anisotropy among the transition metal ions and has been shown previously to be an excellent metal probe in metalloproteins (Bertini and Luchinat 1984). Addition of CoCl₂ into the solution of 0.1 mM ¹⁵N-A28C-2V-8HQ generated a new set of signals in the ¹⁵N-HSQC spectrum with increasing intensities as the concentration of cobalt ion

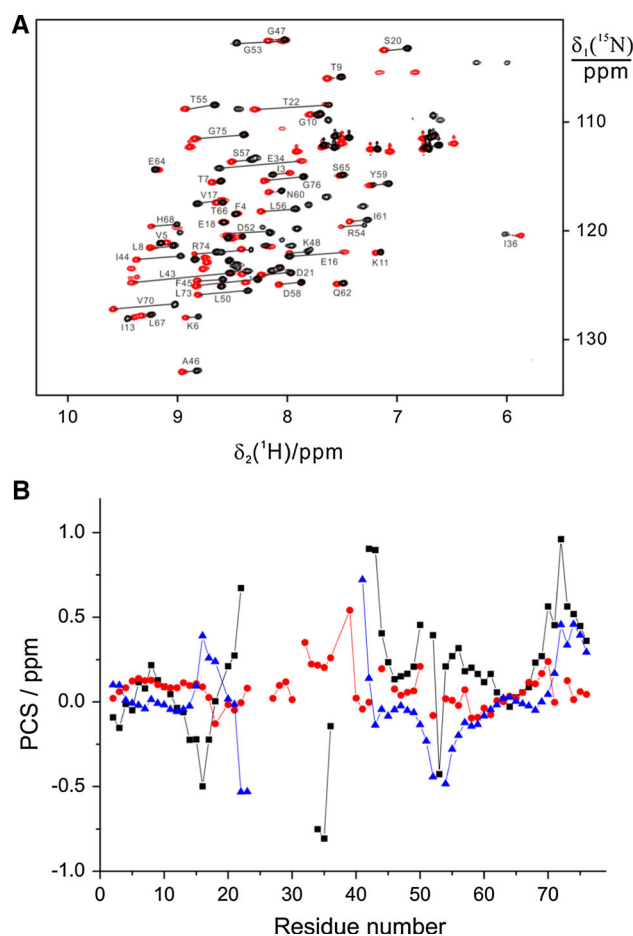


Fig. 3 **a** Superimposition of ¹⁵N-HSQC spectra of a 0.1 mM uniformly ¹⁵N-labeled ubiquitin E24H/A28C-2V-8HQ in the presence of one equivalent Zn(II) (black) and one equivalent Co(II) (red). **b** PCSs of protein backbone amide protons generated by Co(II) in complex with ubiquitin 2V-8HQ adducts of T22C (circles), A28C (triangles), E24H/A28C (squares). The PCSs were calculated as the chemical shift differences between paramagnetic and diamagnetic samples using Zn(II) as the diamagnetic reference

increased. The association–dissociation rate between the metal bound and unbound protein complexes was slow on the NMR time scale, indicating the formed metal complex was stable. There was only a single paramagnetic species corresponding to the complex formed between the protein-2V-8HQ adduct and Co(II) ion during the titration. Similarly, only a single paramagnetic species was observed for the T22C-2V-8HQ and E24H/A28C-2V-8HQ adducts upon addition of Co(II). The A28C-2V-8HQ and E24H/A28C-2V-8HQ adducts complexed with Co(II) experienced significantly larger chemical shift perturbations than T22C-2V-8HQ (Fig. 3 and Fig S3), and therefore we mainly focus on the A28C-2V-8HQ and E24H/A28C-2V-8HQ conjugates in the following. Exchange between Mn(II), Co(II), Ni(II), Cu(II) and Zn(II) complexes of ubiquitin-2V-8HQ was also slow as observed in the ¹⁵N-HSQC spectra.

Binding affinity measurement of ubiquitin-2V-8HQ with transition metal ions

The association constants between transition metal ions and protein-2V-8HQ adducts are difficult to measure by NMR due to slow exchange between the bound and unbound states of the protein. Therefore the thermodynamic stabilities of protein-2V-8HQ complexed with transition metal ion were analyzed by isothermal titration calorimetry (ITC) (Fig S4). In 20 mM MES buffer at pH 6.4 and 289 K, the binding constants of Co(II) and Ni(II) were determined by ITC measurement. The interactions of Mn(II), Cu(II) and Zn(II) ions with protein-2V-8HQ did not result in a sigmoidal titration curve and the titration curves of Mn(II), Cu(II) and Zn(II) failed to yield the binding constants under the conditions used for Co(II) and Ni(II). Despite the fact that A28C-2V-8HQ and E24H/A28C-2V-8HQ showed slow exchange between free protein and metal complex, they differed greatly in binding affinity with Co(II) and Ni(II) ions. The determined association constants, K_a , of E24H/A28C-2V-8HQ for Ni(II) and Co(II) are 4.8×10^5 and $4.0 \times 10^5 \text{ M}^{-1}$, respectively, and are almost ten times larger than those of A28C-2V-8HQ ($6.7 \times 10^4 \text{ M}^{-1}$ with Ni(II) and $4.9 \times 10^4 \text{ M}^{-1}$ with Co(II)). The change of Glu 24 to His 24 in the ubiquitin-2V-8HQ adducts thus increased the binding affinity for the transition metal ions by almost an order of magnitude, supporting the notion that the sidechain imidazole is a preferred ligand over a carboxylate.

Paramagnetic anisotropy of Co(II) complexed with ubiquitin-2V-8HQ

The paramagnetic properties of transition metal ions bound to protein-2V-8HQ conjugates were analyzed by high resolution NMR spectroscopy. PCSs were determined from the chemical shift differences between the paramagnetic and diamagnetic species (Fig. 3, Fig. S3 and Fig. S5), using Zn(II) as the diamagnetic reference. Ni(II) has been extensively applied in structural biology due to its anisotropic paramagnetic properties (Jensen and Led 2006; Jensen et al. 2004), however, its complex with protein-2V-8HQ produced only small chemical shift changes in the present study. As expected, the NMR resonances were also much less attenuated by PREs compared with Co(II), Mn(II) and Cu(II) because most cross-peaks were observable in ^{15}N -HSQC spectra even for residues close to the ligation site (Fig S5). The negligible chemical shift changes and lack of cross-peak attenuation observed with Ni(II) in the ubiquitin-2V-8HQ conjugates is likely due to the formation of a square-planar complex which is diamagnetic because the electrons occupying the 3d orbitals are fully paired. The diamagnetic properties of the protein-2V-8HQ-Ni(II)

complexes were similar to that of a previously published histidine-coordinated protein complex (Jones et al. 2005).

Figure 3 shows sizable PCSs induced by the Co(II) complex that produces larger chemical shift changes (up to 0.8 ppm) than any of the other transition metal ions. Similarly, a large number of residues are observable in the ^{15}N -HSQC spectra of ubiquitin-2V-8HQ complexed with other metal ions. In the case of the copper(II) complex, proton spins within 10 \AA of the paramagnetic center are generally inaccessible to NMR measurement (Arnesano et al. 2003), but nonetheless a large number of residues are observable in ^{15}N -HSQC spectra of the ubiquitin-2V-8HQ-Cu(II) complex (Fig. 4). In the case of Mn(II), which causes stronger PRE than Cu(II), several peaks in the ^{15}N -HSQC spectra of the ubiquitin-2V-8HQ Mn(II) complex display line broadening, yet the same signals as with the copper complex can be observed clearly.

The paramagnetic anisotropy was analyzed for the protein complexes of Co(II) as the PCSs produced by Cu(II) are small. As shown in Fig. 3b, the T22C-2V-8HQ conjugate in complex with cobalt(II) generated smaller PCSs than those of the A28C-2V-8HQ and E24H/A28C-2V-8HQ conjugates. The different sizes of PCSs in the three conjugates indicate different degrees of averaging. Since mobility of either the coordination to the paramagnetic center or of the tether linking 2V-8HQ and protein will result in paramagnetic averaging, the sizes of the PCSs and RDCs are sensitive to this flexibility. In the structure of ubiquitin, Thr22 resides at the start of the first α -helix and Ala28 is in the middle of the same helix. Smaller PCSs in the T22C-2V-8HQ-Co(II) complex indicate a stronger averaging of paramagnetic effects due to flexible coordination of the cobalt ion, implying that coordination with the protein sidechain probably does not sufficiently restrain the paramagnetic center in this case.

In general, the PCS of a nuclear spin is described by Eq. 1,

$$PCS = \frac{1}{12\pi r^3} [\Delta\chi_{ax}(3\cos^2\theta - 1) + 1.5\Delta\chi_{rh}\sin^2\theta\cos 2\phi] \quad (1)$$

where r , θ , and ϕ are the polar coordinates of the nuclear spin relative to the principal axes of the magnetic susceptibility anisotropy tensor $\Delta\chi$, and $\Delta\chi_{ax}$ and $\Delta\chi_{rh}$ are the axial and rhombic components of $\Delta\chi$ -tensor, respectively. It is evident that reliable tensors can be determined provided that the paramagnetic center is accurately defined. Using the program Numbat (Schmitz et al. 2008), the magnetic susceptibility tensor was determined by using the PCS data of backbone amide protons and the crystal structure of ubiquitin (Ramage et al. 1994) or the RDC refined NMR structure (Maltsev et al. 2014), respectively. Both structures gave similar results (Table 1). Excellent

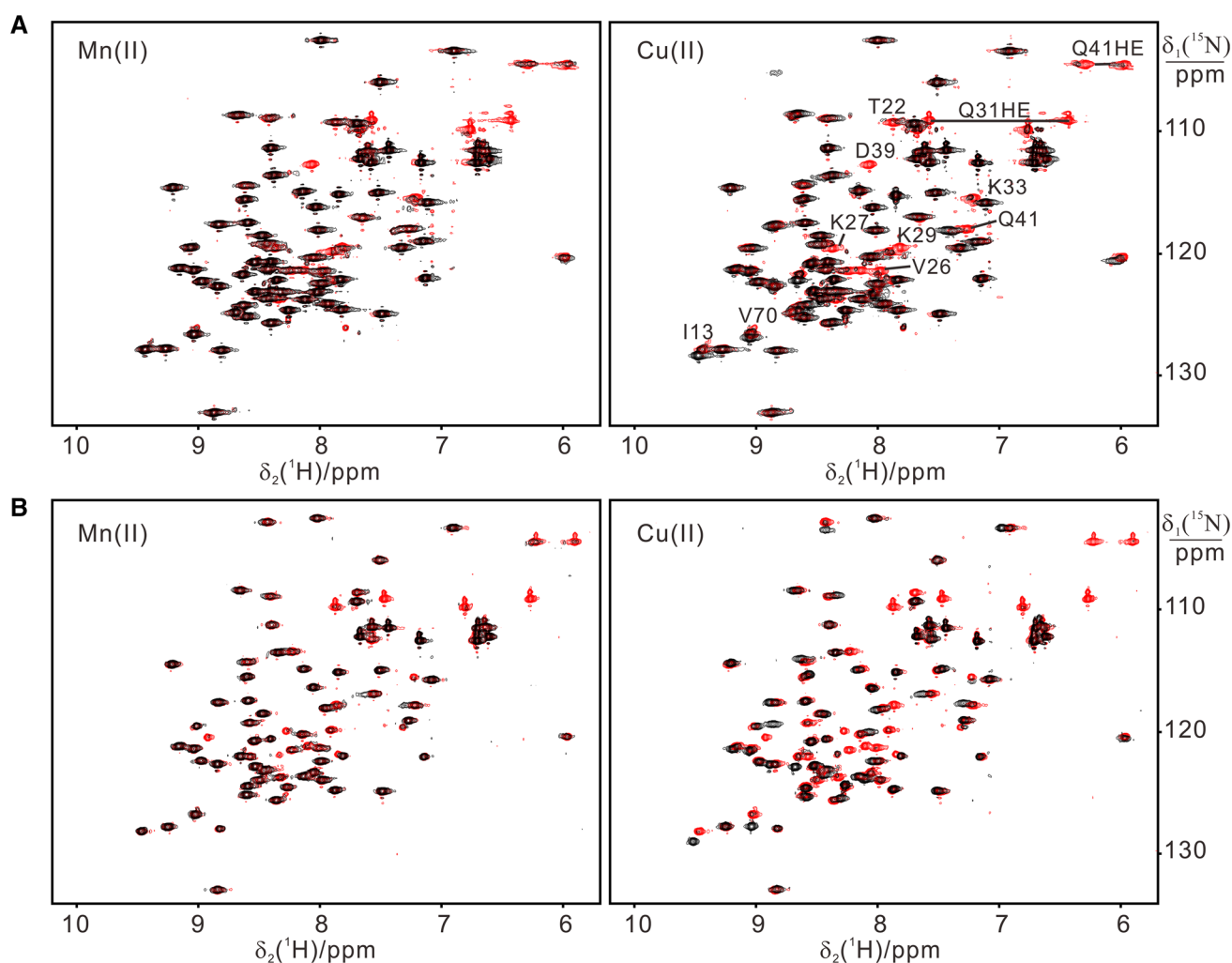


Fig. 4 Superimposition of ^{15}N -HSQC spectra of ubiquitin-2V-8HQ (red) complexed with Mn(II) and Cu(II). **a** 0.1 mM A28C-2V-8HQ complexed with 0.1 mM Mn(II) and Cu(II) (black). **b** 0.05 mM E24H/A28C-2V-8HQ complexed with 0.05 mM Mn(II) and Cu(II) (black)

Table 1 $\Delta\chi$ -tensor parameters of ubiquitin-2V-8HQ complexes with Co(II) ion

	A28C	E24H/A28C	T22C
$\Delta\chi_{ax}$	8.3 (7.5)	-10.3 (-8.6)	-2.1 (-2.2)
$\Delta\chi_{rh}$	5.0 (4.4)	-3.7 (-2.8)	-0.6 (-0.8)
α	64.1 (117.3)	79.4 (56.9)	90.6 (134.8)
β	23.7 (92.3)	141.2 (90.1)	35.7 (78.3)
γ	91.2 (167.8)	66.5 (31.9)	85.5 (174.6)

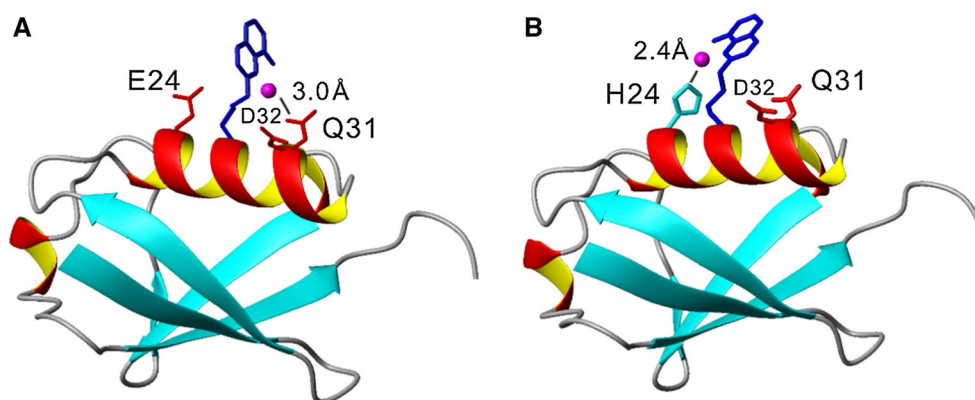
The tensor parameters are in units of 10^{-32} m^3 and were determined by fitting the PCS data of backbone amide protons to the crystal structure of ubiquitin (PDB code: 1UBI) using program Numbat (Schmitz et al. 2008). For comparison, the tensor parameters by using the RDC refined ubiquitin structure (PDB code: 2MJB, first conformer) are shown in brackets

correlations between the experimental PCS and back-calculated data are observed (Fig S6), indicating that the calculated tensors are reliable.

The magnetic anisotropy determined for Co(II) bound to the ubiquitin A28C-2V-8HQ adduct (Table 1) is close to that of high-spin cobalt(II) in the blue copper protein azurin (Donaire et al. 1998), where the cobalt forms a tetrahedral coordination complex. The cobalt complex in A28C-2V-8HQ is also similar to the West Nile virus NS2B-NS3 protease (Nguyen et al. 2011), where the cobalt binds to a genetically encoded bipyridylalanine assisted by additional protein sidechains. These two high-spin cobalt complexes produce similar magnitude of the $\Delta\chi$ -tensors.

The Co(II) complex of the E24H/A28C-2V-8HQ adduct generated larger PCSs than ubiquitin A28C-2V-8HQ, and correspondingly the determined $\Delta\chi$ -tensor is also larger (Table 1). More importantly, the two cobalt complexes produced different $\Delta\chi$ -tensors both in magnitudes and orientations. This confirms that the single point mutation of E24H is effective in changing the paramagnetic tensor significantly, suggesting different coordinating modes of

Fig. 5 Structural view of ubiquitin-2V-8HQ complexed with Co(II). **a** A28C-2V-8HQ. **b** E24H/A28C-2V-8HQ. The calculated paramagnetic center is identified by a sphere (magenta) and the distances of metal ion to sidechain amide oxygen and nitrogen of imidazole is indicated by a solid line. The structure was determined by PyParaTool



Co(II) complexes in these two protein adducts. From structure modeling of the tag based on the PCS data it is evident that the imidazole of histidine is coordinated to cobalt in the E24H/A28C-2V-8HQ conjugate (Table 1; Fig. 5b).

Error analysis of the paramagnetic tensors was performed by random selection of 80 % of the PCSs data to fit the crystal structure (Ramage et al. 1994; PDB code: 1UBI) and RDC-refined NMR structure (Maltsev et al. 2014; PDB code: 2MJB). Both A28C-2V-8HQ and E24H/A28C-2V-8HQ adducts complexed with Co(II) gave high precision in tensor determinations, and the outcomes of 100 calculations are shown in Fig. S7. The Sanson-Flamsteed projections demonstrate that the paramagnetic tensors of Co(II) complexes of A28C-2V-8HQ and E24H/A28C-2V-8HQ differ greatly in orientations (Fig S7). The different coordination modes of E24H imidazole and E24, Q31 or D32 sidechain carboxylate or amide are likely to cause different paramagnetic anisotropy and change the angles of the principal axes of the $\Delta\chi$ -tensors. In the case of T22C-2V-8HQ, the fitted paramagnetic tensors are more spread, suggesting that the paramagnetic tensors are less reliable. This is because in the T22C-2V-8HQ conjugate the dual coordination by 8HQ and a protein sidechain (probably E24) is ill-matched to restrict the flexibility of paramagnetic center, resulting in a loosely coordinated metal complex. In the structure of ubiquitin, A28 resides in the middle of the first α -helix and between the acidic residues E24 and D32 that reside in the $i - 4$ and $i + 4$ positions, respectively. In addition, Q31 is located in the $i + 3$ position. In the case of the A28C-2V-8HQ conjugate, the calculated paramagnetic center has a distance of 5.4 Å to the sidechain oxygen of D32 but with a shorter distance of about 3.0 Å to the sidechain oxygen of Q31. In contrast, the cobalt ion is closer to the side-chain of residue E24 with a distance of 5.0 Å in the complex with E24H/A28C-2V-8HQ. In both protein conjugates, the Q-factors are very small (Fig S6). These results indicate that Q31 and E24H are involved in coordinating the cobalt(II) ion in the A28C-2V-8HQ and E24H/A28C-2V-8HQ adducts, respectively.

To obtain a structural view of the metal complex with respect to the protein, explicit tag coordinates were calculated using PyParaTool (Stanton-Cook et al.). For the cobalt complex of A28C-2V-8HQ, the determined metal position resides close to the sidechain oxygen of Q31 with a distance of 3.0 Å, suggesting Q31 instead of D32 is coordinated to the cobalt ion in addition to 8HQ (Fig. 5). In the structure of E24H/A28C-2V-8HQ, the sidechain of histidine is more favorable to bind the cobalt ion. The calculated distance of the cobalt ion to the sidechain nitrogen of His24 is 2.4 Å as shown in Fig. 5b, which is in good agreement with the typical coordination distance of Co(II). These results are in agreement with a fluorescence analysis of the zinc complex. The preferential coordination of Zn(II) to histidine over carboxylate or amide sidechains results in stronger fluorescence in E24H/A28C-2V-8HQ than A28C-2V-8HQ (Fig S8). It is noted that in the T22C-2V-8HQ and A28C-2V-8HQ adducts the pair of residues at positions i and $i + 4$, where i is Cys and $i + 4$ is Glu or Asp, is not an ideal combination to restrain the transition metal ion. However, a segment in the helix, where residue i is Cys, $i + 3$ is Gln or Glu or $i - 4$ is His, is preferred to immobilize the 2V-8HQ tag.

Comparison of PCSs and RDCs measured for Co(II) complexes of ubiquitin-2V-8HQ adducts

Mobility of a paramagnetic tag generally arises from chemical bond reorientations of the metal-chelating groups and from motions of the linker between protein and paramagnetic tag. The flexibility of the tag will cause different averaging in RDCs and PCSs, because PCSs are distance dependent whereas RDCs are not. RDCs are more sensitive to the tag mobility than PCSs (Shishmarev and Otting 2013). To elucidate the flexibility of the tag in ubiquitin-2V-8HQ, RDCs of protein backbone amides were measured for the Co(II) complex of ubiquitin E24H/A28C-2V-8HQ. The alignment tensor was calculated by fitting the RDCs to the crystal structure of ubiquitin (PDB code:

Table 2 Comparison of alignment tensor and $\Delta\chi$ -tensor parameters of ubiquitin E24H/A28C-2V8HQ complexed with Co(II)

	$10^4 A_{ax}^a$	$10^4 A_{rh}^a$	$10^4 A_{ax}^b$	$10^4 A_{rh}^b$
Co(II)	2.2	1.5	2.6 (2.2)	0.9 (0.7)

All data recorded at 25 °C and 600 MHz ^1H NMR frequency

^a Alignment tensor determined using Module (Dosset et al. 2001). Only RDCs of residues in regular secondary structure elements were used in the fit (residues 2–8, 12–17, 41–45, 47–50, 65–70)

^b Alignment tensor predicted from the $\Delta\chi$ -tensor values of Table 1 using $A_{ax,rh} = \frac{B_0^2}{15kT\mu_0} \Delta\chi_{ax,rh}$

IUBI) using the program Module (Dosset et al. 2001) (Table 2). Similar results were obtained with the NMR structure (Maltsev et al. 2014). The alignment tensors determined from RDCs and back-calculated from PCSs were quite similar (Table 2). The result is consistent with the FANTEN calculation (Rinaldelli et al. 2014) that can directly determine the $\Delta\chi$ -tensor parameters from the input of RDC values (Table S1). These data confirm that 2V-8HQ is a rigid cobalt binding tag, which immobilizes the paramagnetic center in a similar way as the published 4MMDPA (Su et al. 2008) and 3MDPA (Man et al. 2010) tags.

PRE analysis of Mn(II) and Cu(II) complexed with 2V-8HQ adducts

PREs are extensively used in structural biology (Clare and Iwahara 2009), but caution must be taken when interpreting PREs because transient non-specific encounters between the paramagnetic center and the protein surface can contribute significant effects, requiring an assessment of whether the presence of free metal ion in the protein sample and non-specific transient associations between the paramagnetic tag and the surface of the protein that contributes to the observations. Several studies have shown that ubiquitin itself binds transition metal ions (Arena et al. 2011; Falini et al. 2008; Arnesano et al. 2011), therefore the PRE effects on ubiquitin-2V-8HQ conjugates were also assessed in this study.

The PRE effects were evaluated by comparison of the changes in cross-peak intensity in ^{15}N -HSQC spectra between the diamagnetic (in the absence of metal ion) and paramagnetic samples. The ubiquitin-2V-8HQ conjugates formed complexes with Mn(II) and Cu(II) ions that were in slow exchange on the NMR time scale. Titration of the paramagnetic ions Mn(II) and Cu(II) into the solution of ubiquitin-2V-8HQ produced different effects on the protein signals. For example, formation of the copper(II) complex with protein not only generated significant PREs but also sizable chemical shift changes for some residues as shown

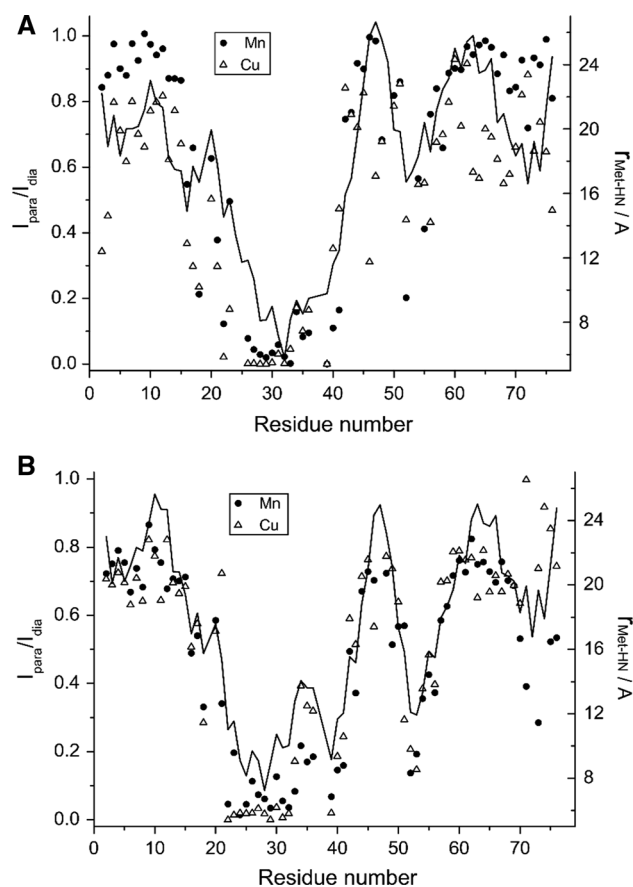


Fig. 6 PREs of protein backbone amide protons detected as peak intensity ratios in the ^{15}N -HSQC spectra of protein samples in the presence and absence of one equivalent paramagnetic Mn(II) (circle) or Cu(II) (triangle). **a** 0.1 mM A28C-2V-8HQ, **b** 0.05 mM E24H/A28C-2V-8HQ. I_{para} and I_{dia} are the cross-peak intensities for the backbone amide protons in the presence and absence of paramagnetic metal ion. The ratio $I_{\text{para}}/I_{\text{dia}}$ is shown on the left and the calculated distances of backbone amide protons from the paramagnetic center, determined by fitting PCS data to the crystal structure of ubiquitin (PDB code: 1UBI), are plotted as a line with the scale shown on the right

in Fig. 4. In contrast, addition of Mn(II) into the solution of protein-2V-8HQ only produced PREs on NMR signals. In general, the residues most affected by PREs were vicinal to the mutation site of A28C, indicating that the paramagnetic center was located near that site. Assuming that Mn(II) and Cu(II) share similar structural modes as Co(II) bound to ubiquitin-2V-8HQ, the metal positions of Mn(II) and Cu(II) were assumed to be the same as that of Co(II) in these complexes. Correlations of peak intensity ratios with respect to the amino acid sequence are shown in Fig. 6. For comparison, the cross-peak attenuations with respect to the distances of backbone amide protons to the paramagnetic center are also shown in Fig. 6. The amide protons within a 10 Å radius of the paramagnetic center

were generally undetectable in the ^{15}N -HSQC spectra of the A28C and E24H/A28C-2V-8HQ adducts complexed with Mn(II) and Cu(II) ions. In the case of the A28C-2V-8HQ conjugate, significant peak attenuations were also observed for the residues Gln2, Ile3 and Gly76 at the N- and C-termini, which are probably due to intermolecular PREs at the protein concentration of 0.1 mM. In general, the peak attenuations were in good agreement with the calculated distances of the amide protons from the paramagnetic center for both Mn(II) and Cu(II) complexes.

For the metal complexes of E24H/A28C-2V-8HQ, the PREs of backbone amide protons correlated particularly well with the distances from the paramagnetic center (Fig. 6b). Compared with A28C-2V-8HQ, the cross-peak attenuations determined for the Mn(II) and Cu(II) complexes with E24H/A28C-2V-8HQ agreed well with the paramagnetic center determined by the PCSs of the Co(II) complex, indicating more similar structural modes associated with the coordination of histidine sidechain than with carboxylates or amides. It should be noted that the C-terminal flexible residues also experienced significant PREs for the complex of Mn(II), whereas the peak attenuations in the Cu(II) complex matched the expectations equally well for these C-terminal residues as for those in the rest of the protein. The effect may have arisen from solvent PREs due to an excess of Mn(II) ion during the titration. In both protein samples, no indication of free paramagnetic ion bound to the protein surfaces as shown previously (Arena et al. 2011; Falini et al. 2008; Arnesano et al. 2011) was found.

Compared with published small paramagnetic tags, such as 4MMDPA (Su et al. 2008), 3MDPA (Man et al. 2010), 4MDPA (Jia et al. 2011), NTA (Swarbrick et al. 2011) and IDA tags (Loh et al. 2015), which are suitable for lanthanide ions, 2V-8HQ is of similar size but has high binding affinity for transition metal ions. In addition, C–S thioether protein conjugates are stable and resistant to reducing reagent and therefore can be used in NMR analyses under reducing conditions. The cobalt(II) coordinated 3MDPA protein adduct reported previously showed significantly smaller paramagnetic tensors compared with A28C-2V-8HQ and E24H/A28C-2V-8HQ, implying a different coordination of 8HQ to cobalt. As lanthanide ions generally have coordination numbers of eight to ten, small lanthanide binding tags do not easily afford strong binding capability and generally fast exchange between protein and protein–metal complex will be observed in NMR spectra, which can result in significant solvent PREs and non-specific association of free metal ion to the protein surface. 2V-8HQ is not suitable for lanthanide ions but its advantage lies in its strong binding affinity for transition metal ions and fluorescent property in complex with a zinc ion, which can be used in fluorescent energy transfer (FRET) measurements. Due to its small size and rigidity, 2V-8HQ

is a useful paramagnetic and fluorescent tag that can be used in structural biology by NMR and fluorescence analysis. Selective modification of a single thiol group may also be possible for a protein containing two or more cysteines, provided that the cysteines have different solvent accessibility and local mobility as those effects will greatly affect the reactivity of protein thiols (Ma et al. 2014).

Conclusions

We show that 8HQ, a well-known transition metal chelator, can be site-specifically attached to a protein in a Michael addition-like thiol-ene reaction. The protein-2V-8HQ conjugates contain a stable thioether tether and show high binding affinities with transition metal ions. The determined paramagnetic tensors of cobalt possess the character of high-spin cobalt(II) complexes. The metal binding affinity can be further enhanced in a helix (Yagi et al. 2013), if i is histidine and $i + 4$ the tagged cysteine. Different paramagnetic tensors can simply be achieved by changing the coordination of the paramagnetic ion by suitable amino acid sidechains in the 2V-8HQ labeled protein. In summary, 2V-8HQ offers an attractive way of coordinating transition metal ions, producing a rigid, stable and small transition metal binding tag that can be used in structural analysis by NMR and also fluorescence spectroscopy.

Acknowledgments Financial support by the 973 program (2013CB910200), the National Science Foundation of China (21473095 and 21273121), and the Australian Research Council (DP120100561 and DP150100383) is greatly acknowledged.

References

- Abragam A, Bleaney B (1970) Electron paramagnetic resonance of transition ions. Oxford University Press, Oxford
- Alacid E, Najera C (2008) Aqueous sodium hydroxide promoted cross-coupling reactions of alkenyltrialkoxysilanes under ligand-free conditions. *J Org Chem* 73:2315–2322
- Arena G, Fattorusso R, Grasso G, Grasso GI, Isernia C, Malgieri G, Milardi D, Rizzarelli E (2011) Zinc(II) complexes of ubiquitin: speciation, affinity and binding features. *Chem Eur J* 17:11596–11603
- Arnesano F, Banci L, Bertini I, Felli IC, Luchinat C, Thompsett AR (2003) A strategy for the NMR characterization of type II copper(II) proteins: the case of the copper trafficking protein CopC from *Pseudomonas syringae*. *J Am Chem Soc* 125: 7200–7208
- Arnesano F, Banci L, Piccoli M (2005) NMR structures of paramagnetic metalloproteins. *Q Rev Biophys* 38:167–219
- Arnesano F, Belviso BD, Caliandro R, Falini G, Fermani S, Natile G, Siliqi D (2011) Crystallographic analysis of metal-ion binding to human ubiquitin. *Chem Eur J* 17:1569–1678
- Bertini I, Luchinat C (1984) High spin cobalt(II) as a probe for the investigation of metalloproteins. *Adv Inorg Biochem* 6:71–111

- Bertini I, Luchinat C (1996) NMR of paramagnetic substances. *Coord Chem Rev* 150:1–243
- Bertini I, Luchinat C (1999) New applications of paramagnetic NMR in chemical biology. *Curr Opin Chem Biol* 3:145–151
- Bertini I, Turano P, Vila AJ (1993) Nuclear magnetic resonance of metalloproteins. *Chem Rev* 93:2833–2932
- Bertini I, Luchinat C, Parigi G (2002) Magnetic susceptibility in paramagnetic NMR. *Prog NMR Spectr* 40:249–273
- Bertini I, Luchinat C, Parigi G, Pierattelli R (2005) NMR spectroscopy of paramagnetic metalloproteins. *Chembiochem* 6:1536–1549
- Bertini I, Luchinat C, Parigi G, Pierattelli R (2008) Perspectives in paramagnetic NMR of metalloproteins. *Dalton* 3782–3790
- Cao C, Chen JL, Yang Y, Huang F, Otting G, Su XC (2014) Selective ^{15}N -labeling of the side-chain amide groups of asparagine and glutamine for applications in paramagnetic NMR spectroscopy. *J Biomol NMR* 59:251–261
- Clore GM, Iwahara J (2009) Theory, practice, and applications of paramagnetic relaxation enhancement for the characterization of transient low-population states of biological macromolecules and their complexes. *Chem Rev* 109:4108–4139
- Donaire A, Salgado J, Moratal JM (1998) Determination of the magnetic axes of cobalt(II) and nickel(II) azurins from ^1H NMR data: influence of the metal and axial ligands on the origin of magnetic anisotropy in blue copper proteins. *Biochemistry* 37:8659–8673
- Dosset P, Hus JC, Marion D, Blackledge M (2001) A novel interactive tool for rigid-body modeling of multi-domain macromolecules using residual dipolar couplings. *J Biomol NMR* 20:223–231
- Falini G, Fermani S, Tosi G, Arnesano F, Natile G (2008) Structural probing of Zn(II), Cd(II) and Hg(II) binding to human ubiquitin. *Chem Commun* 5980–5962
- Geraldes CF (1993) Lanthanide shift reagents. *Methods Enzymol* 227:43–78
- Geraldes CF, Luchinat C (2003) Lanthanides as shift and relaxation agents in elucidating the structure of proteins and nucleic acids. *Met Ions Biol Syst* 40:513–588
- Gochin M (1998) Nuclear magnetic resonance characterization of a paramagnetic DNA-drug complex with high spin cobalt; assignment of the ^1H and ^{31}P NMR spectra, and determination of electronic, spectroscopic and molecular properties. *J Biomol NMR* 12:243–257
- Huang F, Pei YY, Zuo HH, Chen JL, Yang Y, Su XC (2013) Bioconjugation of proteins with a paramagnetic NMR and fluorescent tag. *Chem Eur J* 19:17141–17149
- Jensen MR, Led JJ (2006) Metal–protein interactions: structure information from Ni(II)-induced pseudocontact shifts in a native nonmetalloprotein. *Biochemistry* 45:8782–8787
- Jensen MR, Lauritzen C, Dahl SW, Pedersen J, Led JJ (2004) Binding ability of a HHP-tagged protein towards Ni^{2+} studied by paramagnetic NMR relaxation: the possibility of obtaining long-range structure information. *J Biomol NMR* 29:175–185
- Jia X, Maleckis A, Huber T, Otting G (2011) 4,4'-Dithiobisdipicolinic acid: a small and convenient lanthanide binding tag for protein NMR spectroscopy. *Chem Eur J* 17:6830–6836
- Johnston WD, Freiser H (1952) Structure and behavior of organic analytical reagents. III. Stability of chelates of 8-hydroxyquinoline and analogous reagents. *J Am Chem Soc* 74:5239–5242
- Jones CE, Klewpatinond M, Abdelraheim SR, Brown DR, Viles JH (2005) Probing copper binding to the prion protein using diamagnetic nickel and ^1H NMR: the unstructured N terminus facilitates the coordination of six copper ions at physiological concentrations. *J Mol Biol* 346:1393–1407
- Koehler J, Meiler J (2011) Expanding the utility of NMR restraints with paramagnetic compounds: background and practical aspects. *Prog NMR Spectr* 59:360–389
- La Mar GN, Horrocks WD, Holm RH (1973) NMR of paramagnetic molecules. Elsevier, Amsterdam
- Lee HS, Spraggon G, Schultz PG, Wang F (2009) Genetic incorporation of a metal-ion chelating amino acid into proteins as a biophysical probe. *J Am Chem Soc* 131:2481–2483
- Li QF, Yang Y, Maleckis A, Otting G, Su XC (2012) Thiol-ene reaction: a versatile tool in site-specific labelling of proteins with chemically inert tags for paramagnetic NMR. *Chem Commun* 48:2704–2706
- Liu X, Li J, Hu C, Zhou Q, Zhang W, Hu M, Zhou J, Wang J (2013) Significant expansion of the fluorescent protein chromophore through the genetic incorporation of a metal-chelating unnatural amino acid. *Angew Chem Int Ed Engl* 52:4805–4809
- Liu WM, Overhand M, Ubbink M (2014) The application of paramagnetic lanthanoid ions in NMR spectroscopy on proteins. *Coord Chem Rev* 273–274:2–12
- Loh CT, Graham B, Abdelkader EH, Tuck KL, Otting G (2015) Generation of pseudocontact shifts in proteins with lanthanides using small “clickable” nitrilotriacetic acid and iminodiacetic acid tags. *Chem Eur J* 21:5084–5092
- Ma FH, Chen JL, Li QF, Zuo HH, Huang F, Su XC (2014) Kinetic assay of the Michael addition-like thiol-ene reaction and insight into protein bioconjugation. *Chem Asian J* 9:1808–1816
- Maltsev AS, Grishaev A, Roche J, Zasloff M, Bax A (2014) Improved cross validation of a static ubiquitin structure derived from high precision residual dipolar couplings measured in a drug-based liquid crystalline phase. *J Am Chem Soc* 136:3752–3755
- Man B, Su XC, Liang H, Simonsen S, Huber T, Messerle BA, Otting G (2010) 3-Mercapto-2,6-pyridinedicarboxylic acid: a small lanthanide-binding tag for protein studies by NMR spectroscopy. *Chem Eur J* 16:3827–3832
- Marley J, Lu M, Bracken C (2001) A method for efficient isotopic labeling of recombinant proteins. *J Biomol NMR* 20:71–75
- Martorana A, Yang Y, Zhao Y, Li QF, Su XC, Goldfarb D (2015) Mn(II) tags for DEER distance measurements in proteins via C–S attachment. *Dalton Trans* 44:20812–20816
- Nguyen THD, Ozawa K, Stanton-Cook M, Barrow R, Huber T, Otting G (2011) Generation of pseudocontact shifts in protein NMR spectra with a genetically encoded cobalt(II)-binding amino acid. *Angew Chem Int Ed* 50:692–694
- Otting G (2008) Prospects for the lanthanides in structural biology by NMR. *J Biomol NMR* 42:1–9
- Otting G (2010) Protein NMR using paramagnetic ions. *Annu Rev Biophys* 39:387–405
- Park SH, Wang VS, Radoicic J, De Angelis AA, Berkamp S, Opella SJ (2015) Paramagnetic relaxation enhancement of membrane proteins by incorporation of the metal-chelating unnatural amino acid 2-amino-3-(8-hydroxyquinolin-3-yl)propanoic acid (HQA). *J Biomol NMR* 61:185–196
- Petitjean A, Kyritsakas N, Lehn JM (2005) Ion-triggered multistate molecular switching device based on regioselective coordination-controlled ion binding. *Chem Eur J* 11:6818–6828
- Pintacuda G, John M, Su XC, Otting G (2007) NMR structure determination of protein–ligand complexes by lanthanide labelling. *Acc Chem Res* 40:206–212
- Qi A, Gross A, Jeschke G, Godt A, Drescher M (2014) Gd(III)-PyMTA label is suitable for in-cell EPR. *J Am Chem Soc* 136:15366–15378
- Ramage R, Green J, Muir TW, Ogunjobi OM, Love S, Shaw K (1994) Synthetic, structural and biological studies of the ubiquitin system: chemically synthesized and native ubiquitin fold into identical three-dimensional structures. *Biochem J* 299:151–158
- Rinaldelli M, Carlon A, Ravera E, Parigi G, Luchinat C (2014) FANTEN: a new web-based interface for the analysis of magnetic anisotropy-induced NMR data. *J Biomol NMR* 61:21–34

- Rodriguez-Castañeda F, Haberz P, Leonov A, Griesinger C (2006) Paramagnetic tagging of diamagnetic proteins for solution NMR. *Magn Reson Chem* 44:S10–S16
- Shishmarev D, Otting G (2013) How reliable are pseudocontact shifts induced in proteins and ligands by mobile paramagnetic metal tags? A modelling study. *J Biomol NMR* 56:203–216
- Schmitz C, Stanton-Cook MJ, Su XC, Otting G, Huber T (2008) Numbat: an interactive software tool for fitting $\Delta\chi$ -tensors to molecular coordinates using pseudocontact shifts. *J Biomol NMR* 41:179–189
- Stanton-Cook MJ, Su XC, Otting G, Huber T. <http://compbio.anu.edu.au/mscook/PPT/>
- Su XC, Man B, Beeren S, Liang H, Simonsen S, Schmitz C, Huber T, Messerle BA, Otting G (2008) A dipicolinic acid tag for rigid lanthanide tagging of proteins and paramagnetic NMR spectroscopy. *J Am Chem Soc* 130:10486–10487
- Swarbrick JD, Ung P, Su XC, Maleckis A, Chhabra S, Huber T, Otting G, Graham B (2011) Engineering of a bis-chelator motif into a protein α -helix for rigid lanthanide binding and paramagnetic NMR spectroscopy. *Chem Commun (Camb)* 47:7368–7370
- Ubbink M, Ejdebäck M, Karlsson BG, Bendall DS (1998) The structure of the complex of plastocyanin and cytochrome f, determined by paramagnetic NMR and restrained rigid-body molecular dynamics. *Structure* 6:323–335
- Yagi H, Maleckis A, Otting G (2013) A systematic study of labelling an α -helix in a protein with a lanthanide using IDA-SH or NTA-SH tags. *J Biomol NMR* 55:157–166
- Yang Y, Li QF, Cao C, Huang F, Su XC (2013) Site-specific labeling of proteins with a chemically stable, high-affinity tag for protein study. *Chem Eur J* 19:1097–1103